Research article

Apomorphine-induced pathway perturbation in MPP⁺-treated SH-SY5Y cells

Jin Hwan Do*

Department of Biomolecular and Chemical Engineering, DongYang University, Yeongju 36040, South Korea

* **Correspondence:** Email: jinhwando@dyu.ac.kr; Tel: +82-54-630-1361; Fax: +82-54-637-2112.

Abstract: Apomorphine (APOM) is a non-selective dopamine agonist for Parkinson's disease (PD). It also offers protection against oxidative stress. Thus, it has been used for treating advanced PD patients who do not respond to levodopa or other dopamine agonists. However, side effects such as orthostatic hypotension, nausea, and fibrotic nodules at the site of APOM injection have been reported after long-term use of APOM in PD patients. To secure the use of APOM for PD treatment without side effect, it is essential to understand the molecular mechanism involved in the action of APOM in PD. In this study, gene expression profile changes by APOM in a PD cell model, i.e., MPP⁺-treated SH-SY5Y cells, were measured at six time points (0, 3, 6, 9, 12, and 24 h) after APOM treatment using a commercial whole-genome expression array. A total of 2249 genes showed significant and differential expression profile. Pathways significantly affected by APOM were estimated using signaling pathway impact analysis (SPIA). In addition, differentially regulated regions within each affected pathway were identified with covariance analysis using a structure equation model.

Keywords: apomorphine; gene expression; structure equation model; signaling pathway anlaysis; SH-SY5Y cells; Parkinson's disease

1. Introduction

Apomorphine (APOM) is a strong antioxidant and free radical scavenger as well as a non-selective dopamine agonist that can stimulate D_1-like (D_1, D_5) and D_2-like (D_2, D_3, D_4) receptors [1]. Due to its bioactivities, APOM has become the first dopamine agonist used to treat patients with

Parkinson's disease (PD). As PD is caused by the loss of dopamine-generating neurons in the central nervous system, increase of dopamine in the brain has been used as a standard strategy for treating PD. Levodopa (l-dihydroxyphenylalanine), a natural dopamine precursor, can cross the blood-brain barrier. It can be converted to dopamine in the brain. Therefore, it has been used as a main drug for initial treatment of PD [2, 3]. However, long-term use of levodopa may cause drug resistance and aggravation of the symptoms [4]. APOM has been used to treat advanced PD patients with persistent and disabling motor fluctuations [5-7]. It has been suggested that APOM's dyskinetic effect might be mediated by excessive activation of afferents to the centromedian-striatopallidal or pallidal-pedunculopontine pathways [8].

Although the neuroprotecive effect of APOM has been demonstrated both *in vivo* and *in vitro* experiments [9,10], the molecular mechanisms involved in the protection remains unclear. Furthermore, long-term use APOM for treatment of PD patients may lead to side effects such as orthostatic hypotension, nausea, and fibrotic nodules at the site of APOM injection [2]. To secure the use of APOM in PD treatment, it is essential to understand the underlying molecular mechanisms involved in the protection of APOM in PD patients. The aim of this study was to identify pathway regions significantly affected by APOM in PD cell model through analyzing two groups of time series microarray data, i.e., APOM treatment group and reference group using a structure equation model (SEM). Human neuroblastoma SH-SY5Y cells were treated with 1-methyl-4-phenyl-pyridium (MPP$^+$) and used as a PD cell model because they mimic many aspects of dopaminergic (DAergic) neuronal death observed in PD [11,12]. MPP$^+$, an active metabolite of 1-methyl-4-phenyl-1, 2, 3, 6-tetrahydropyridine (MPTP), is taken up by DAergic neurons via dopamine and noradrenaline transporters, resulting in inhibition of complex I of the mitochondrial membrane potential and formation of reactive oxygen species (ROS) [13,14]. As mitochondrial complex I deficiency has long been implicated in the pathogenesis of PD [15], MPP$^+$ treated SH-SY5Y cells have been extensively used as PD cell model. We investigated gene expression profile of SH-SY5Y cells co-treated by APOM and MPP$^+$ at six time points (0, 3, 6, 9, 12, and 24 h) with a commercial whole-genome expression array. To examine the effect of APOM in MPP$^+$-treated SH-SY5Y cells, a reference without APOM treatment was needed for comparison. It has been reported that the genome-wide gene expression data of MPP$^+$-treated SH-SY5Y cells at 0 (control), 3, 6, 9, 12, and 24 h without APOM treatment [12]. Therefore, these expression data were used as reference. The treatment with APOM to MPP$^+$-treated SH-SY5Y cells resulted in significant expression profile changes for a total of 2249 genes. Signaling pathway impact analysis (SPIA) for these 2249 genes were performed and identified KEGG (Kyoto Encyclopedia of Genes and Genomes) pathways significantly affected by APOM, including endoplasmic reticulum (ER) protein processing pathway, fanconi anemia pathway, colorectal cancer, pathogenic *Escherichia coli* infection, cell cycle, and TGF-beta signaling pathway. Covariance structure analysis of these perturbed pathways using SEM identified differentially regulated regions, i.e., significant modules within them. Significant modules might be closely related to the molecular function of APOM in PD cell model. Therefore, our results might improve the understanding of neuroprotective mechanisms of APOM in PD caused by the loss of DAergic neurons.

2. Materials and Methods

2.1. Cell culture and co-treatment of SH-SY5Y cells with MPP+ and APOM

Human neuroblastoma SH-SY5Y cells (ATCC CRL-2266) were cultured at 37 °C in 5% CO$_2$ and 95% air in a humidified incubator. They were maintained in Dulbecco's modified Eagle's Medium

(DMEM, Sigma-Aldrich, St. Louis, MO, USA) supplemented with 10% fetal bovine serum (FBS, Gibco BRL, Grand Island, NY, USA), 100 units/mL penicillin, and 100 mg/mL streptomycin. Freshly prepared APOM and MPP^+ were added simultaneously to 100 mm^2 cell culture dishes (Corning, Cambridge, MA, USA) plated with 1×10^6 cells followed by incubation at 37 °C for 0 (control), 3, 6, 9, 12 and 24 h, respectively. The concentrations of APOM and MPP^+ in the cultures were 10 μM and 1 mM, respectively. Control and treatment experiments were repeated three times.

2.2. RNA extraction and microarray experiment

At each time point after co-treatment with APOM and MPP^+, cells were harvested and total RNAs were extracted using TRIzol® (Invitrogen Life Technologies, USA). RNAs were purified using RNeasy columns (Qiagen, USA) according to the manufacturers' protocol. The purity and integrity of the extracted RNA were examined with denaturing gel electrophoresis, optical density comparison of 260/280 ratio, and Agilent 2100 Bioanalyzer (Agilent Technologies, USA). Microarray experiment was performed for the extracted RNA according to protocols described in Choi et al. [16]. Briefly, 550 ng of the extracted total RNA was reverse-transcribed to first-strand cDNA using a T7 oligo (dT) primer. These first-stand cDNA was then converted to double stranded cDNA (ds-cDNA). The resulting ds-cDNA was employed as template for *in vitro* transcription to prepare labeled cRNA with biotin-NTP. Labeled cRNA (750 ng) was then hybridized to each human HT-12 expression v.4 bead array at 58 °C for 16–18 h according to the manufacturer's instructions (Illumina, Inc., San Diego, USA). Detection of the array signal was carried out using Amersham fluorolink streptavidin-Cy3 (GE Healthcare Bio-Sciences, Little Chalfont, UK) following the bead array manual. Arrays were scanned using Illumina bead array Reader confocal scanner according to the manufacturer's instructions. A total of 18 bead arrays were used for three controls (before treatment) and three samples at each time point (3, 6, 9, 12, and 24 h) after co-treatment with APOM and MPP^+.

2.3. Normalization of microarray data

After microarray data were exported using Illumina GenomeStudio software v2011.1, values of probe signal were log2 transformed and normalized using the function of *lumiN()* from the R package *lumi* [17]. Since the Illumina BeadChip employed in this study was a single-channel array, quantile normalization was chosen. After the normalization, signals under the detection limit were replaced with missing values. Probes with two missing values for the three replicates were filtered out.

2.4. Reference microarray data

To identify perturbed pathways after the addition of APOM to MPP^+-treated SH-SY5Y cells, gene expression data of MPP^+-treated SH-SY5Y cells from the study of Kim et al. [12] were used as reference, including time series microarray data at the control (before MPP^+ treatment) and 3, 6, 9, 12, and 24 h after exposure to 1 mM of MPP^+.

2.5. Selection of genes with differential expression profiles between two time series of microarray data

To select genes showing differential expression profile from two time-series microarray data, *maSigPro* bioconductor package was employed [18]. This program uses a two-step regression approach to identify DEGs in time series microarray data. A global model was adjusted in the first step

whereas the application of variable selection strategy was made to identify significant profile differences between two groups under comparison in the second step. Before comparing expression profiles between two groups of microarray data, log2 ratio of treated sample versus untreated sample (control) was calculated for each group of the microarray data. Microarray data from the study of Kim et al. [12] were used as data for the reference group. Genes showing differential expression profiles were considered significant genes. Enriched GO terms in the set of significant genes were explored with the function *enrichGO()* in the R package *clusterProfiler* [19].

2.6. Identification of perturbed pathways with SPIA

To identify affected pathways by APOM addition to MPP$^+$-treated SH-SY5Y cells, an R package called *SPIA* [20] was employed. This program can find significantly affected pathways based on two types of evidence captured by two independent probability values, P_{NDE} and P_{PERT}. P_{NDE} captures the significance of a given pathway P_i as provided by an over-representation analysis of the number of DEGs observed in the pathway whereas P_{PERT} captures a total perturbation of the pathway and is estimated in a bootstrapping process where both pathway and the number of DEGs per pathway are maintained. Global probability P_G was used for pathway ranking. It was estimated with the following equation:

$$P_G = c_i - c_i \cdot \ln(c_i)$$

where $c_i = P_{NDE}(i) \cdot P_{PERT}(i)$. The net perturbation accumulation at the level of each gene i (g_i), $Acc(g_i)$, was calculated using the following equation:

$$Acc(g_i) = \sum_{j=1}^{n} \beta_{ij} \frac{PF(g_i)}{N_{ds}(g_j)}$$

where β_{ij} was the strength of the interaction between genes g_i and g_j. In this study, the value of β was $+1$ for activation and -1 for inhibition. $PF(g_i)$ was the perturbation factor of gene g_i whereas $N_{ds}(g_j)$ was the number of down-stream genes of gene g_j. Activation/inhibition of pathway was decided by the sign of the total net accumulated perturbation in the pathway: $t_A = \sum_i Acc(g_i)$.

2.7. Construction of the shortest path model for perturbed pathways

After identifying pathways affected by APOM addition to MPP$^+$ treated SH-SY5Y cells, connected structures of DEGs within them were assessed by considering each pathway as a directed graph with the function *get.shortest.paths()* of the R package *igraph* [21]. Each node and edge in the shortest path could not be presented for more than once. Self-loops were excluded but feed-backs and cycles were kept. Non-DEGs might be included in the shortest paths linking DEGs to allow the discovery of genes that are not DEGs but can be important for their mediating roles. The shortest path model (SPM) for each perturbed pathway was constructed by merging all of shortest paths among DEGs for the corresponding pathway as shown in our previous work [22].

2.8. Modularity measurement of SPM

The modularity of SPM for each perturbed pathway was calculated with the following equation:

$$Q = \frac{1}{2m} \sum_{i,j} A_{ij} - \frac{k_i k_j}{2m} \delta(c_i, c_j)$$

Where m is the number of edges, A_{ij} is the element of the i-th row and j-th column of the A adjacency matrix, k_i and k_j are the degree of i and j, respectively, c_i and c_j are component of i and j, respectively. The sum includes over all i and j pairs of vertices, and $\delta(x, y)$ is 1 if $x = y$ and 0 otherwise [23]. Modules within each SPM were detected by using the function *walktrap.community()* in the R package *igraph* [21], which could find densely connected subgraphs in a graph via random walks. If the value of modularity is greater than 0.35, each module in the SPM is considered separately.

2.9. Evaluation of module/SPM with SEM

To examine if a module or SPM are statistically significant by the addition of APOM in MPP$^+$-treated SH-SY5Y cells, they were evaluated with SEM, as in our previous work [22]. Briefly, a module or SPM are considered to have casual relationships among variables such as structure of SEM where all variables can be represented as a system of linear equation:

$$Y_i = \sum_{j \in pa(i)} \beta_{ij} Y_j + U_i \quad i \in V$$

With a covariance structure:

$$\text{cov}(U_i, U_j) = \begin{cases} \psi_{ij} & \text{if } i = j \text{ or } j \in sib(i) \\ 0 & \text{otherwise} \end{cases}$$

Every i^{th} node in the set of variables V are characterized by uni-directional relationships with its "parents" *pa(i)* via path coefficients (β_{ij}). The covariance structure can delineate the bi-directional relationships between the ith node (U_i) and its "siblings" *sib(i)*, as quantified by their covariance (ψ_{ij}). The parameters $\theta = (\beta_{ij}; \psi_{ij})$ in SEM were estimated by Maximum Likelihood Estimation (MLE) with the R package *lavaan*. After parameter estimation of a module/SPM, the significant module/SPM was detected with the following omnibus test:

$$H_0 : \sum\nolimits_1(\theta) = \sum\nolimits_2(\theta) \quad \text{vs.} \quad H_1 : \sum\nolimits_1(\theta) \neq \sum\nolimits_2(\theta)$$

Where $\sum_1(\theta)$ and $\sum_2(\theta)$ are model-implied covariance matrices of control and APOM added samples in MPP$^+$-treated SH-SY5Y cells, θ indicates the model parameter. A statistically significant module/SPM is determined by comparison of the likelihood ratio test (LRT) Chi-square (χ^2) values at a given degree of freedom. When the *p*-value in the Chi-square test is less than 0.05, the module/SPM is considered as statistically significant.

3. Results

3.1. Identification of genes with differential expression profiles

Gene expression profiles of SH-SY5Y cells co-treated with APOM and MPP$^+$ were determined with Illumina whole-genome array (human HT-12 expression v.4 bead array) using 47,231 probes. A total of 18 arrays were employed for the examination of gene expression profile at six time points (0, 3, 6, 9, 12, and 24 h) with three replicates for each time point. After log2 transformation, probe signals were normalized with quantile normalization. Log2 ratio (co-treated sample with APOM and MPP$^+$ vs. control sample at 0 h) was obtained by subtraction of the average of normalized log2 values of three control arrays from normalized log2 value of each time point. When a gene had multiple probe IDs, the average value was assigned to the gene. Of 47,321 probes, only 32,421 probes with unique gene name were considered. To explore gene expression profile changes by the addition of APOM to MPP$^+$-treated SH-SY5Y cells, gene expression data of MPP$^+$-treated SH-SY5Y cells were required as reference. Thus, we employed the microarray data from the work of Kim et al. [12] as reference (see Materials and Methods section for details).

To identify genes showing differential expression profile between the two groups (APOM added group and reference group), a bioconductor package *maSigPro* [18] was employed using a two-regression step approach. In the first step, a global regression model was adjusted with all the defined variables to detect differentially expressed genes (DEGs). In the second step, a variable selection strategy was applied to examine differences between groups and identify statistically significant profiles. When the *p*-value threshold associated to the *F*-Static in general regression model was 0.05, the number of DEGs in the first step was 9395. In the second step, 2249 genes of these 9395 DEGs were found to have significantly differential expression profiles between the APOM added group and the reference group (adjusted *p*-value < 0.05). In this study, genes showing differential expression profiles were considered as significant genes. Their expression profiles are shown in Figures 1 and 2 using the clustering and plotting functions available in the *maSigPro*. In Figure 1, horizontal axis represents the array of reference and APOM added group at different time point. Replicate of each array was marked with a number. The vertical axis represents expression value (log2 ratio). A positive/negative value indicates up-/down-regulation, respectively. A value of 0 means no expression change. Clear contrast in expression profiles between the APOM added group and the reference group was observed in cluster 1. Genes in cluster 1 tended to be up-regulated in the APOM added group. However, they were not changed at expression level or down-regulated in the reference group. For easy comparison of their expression profiles between the two groups, average expression profiles were shown in Figure 2. The three values at each time point corresponded to the three replicates. Red and green lines represent the average expression profiles of the reference and the APOM added group, respectively. In the APOM added group, genes in cluster 1 and 3 tended to be up-regulated while genes in cluster 2 and 4 tended to be down-regulated at early stage.

To catch functional characteristic of each cluster genes, enriched gene ontology (GO) terms were examined with the function *enrichGO* in the R package *clusterProfiler* [19]. With a cutoff *q*-value of 0.05, GO terms such as GO:0036297 (interstrand cross-link repair) and GO:0022616 (DNA strand elongation) were significantly enriched in cluster 1 whereas GO terms such as GO:0009185 (ribonucleoside diphospahte metabolic process), GO:0019320 (hexose catabolic process), and GO:0006096 (glycolytic process) were significantly enriched in cluster 3. The up-regulation of genes in cluster 1 and 3 might have contributed to resistance against DNA damage and cellular metabolic deactivation resulted from MPP$^+$ toxicity. No significantly enriched GO terms were detected for cluster 2 or 4. Top 15 genes of each cluster ranked by *p*-value are shown in Table 1.

Cluster 1 (903 genes)

Cluster 2 (404 genes)

Cluster 3 (145 genes)

Cluster 4 (797 genes)
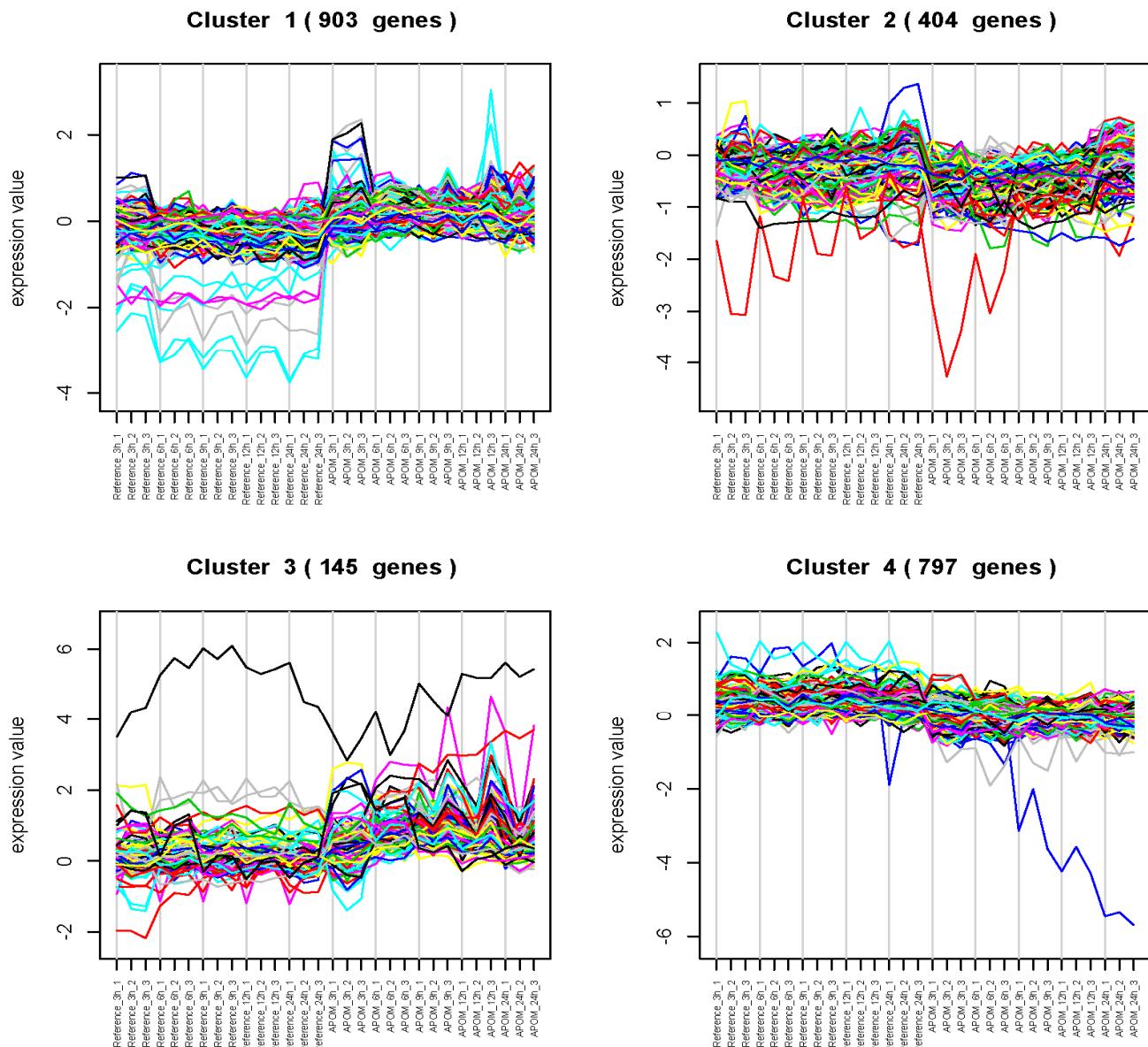
Figure 1. Expression profiles of significant genes in four clusters for the reference group and the APOM added group.

Table 1. Top 15 genes of each cluster ranked by *p*-value among significant genes showing differential profiles between the APOM added group and the reference group.

Group	Gene	Description	*p*-value
1	EGR2	Early growth response 2 (Krox-20 homolog, Drosophila) (EGR2), mRNA.	5.49E−25
	NR4A3	Nuclear receptor subfamily 4, group A, member 3 (NR4A3), transcript variant 3, mRNA.	3.93E−22
	FOSB	FBJ murine osteosarcoma viral oncogene homolog B (FOSB), mRNA.	6.58E−20
	SRF	Serum response factor (c-fos serum response element-binding transcription factor) (SRF), mRNA.	1.99E−18
	NPAS4	Neuronal PAS domain protein 4 (NPAS4), mRNA.	2.50E−18

|			
	EGR1	Early growth response 1 (EGR1), mRNA.	1.19E−16
	GINS2	GINS complex subunit 2 (Psf2 homolog) (GINS2), mRNA.	5.86E−16
	PDCL3	Phosducin-like 3 (PDCL3), mRNA.	9.04E−16
	ZNF503	Zinc finger protein 503 (ZNF503), mRNA.	9.41E−16
	HAUS8	HAUS augmin-like complex, subunit 8 (HAUS8), transcript variant 1, mRNA.	1.05E−15
	KLF6	Kruppel-like factor 6 (KLF6), transcript variant 2, mRNA.	1.32E−15
	DUSP1	Dual specificity phosphatase 1 (DUSP1), mRNA.	4.41E−15
	SLC30A1	Solute carrier family 30 (zinc transporter), member 1 (SLC30A1), mRNA.	4.49E−15
	MYADM	Myeloid-associated differentiation marker (MYADM), transcript variant 4, mRNA.	6.05E−15
	ARC	Activity-regulated cytoskeleton-associated protein (ARC), mRNA.	7.41E−15
2	TM4SF4	Transmembrane 4 L six family member 4 (TM4SF4), mRNA.	2.09E−23
	EFNA1	Ephrin-A1 (EFNA1), transcript variant 1, mRNA.	9.91E−20
	ARID5B	AT rich interactive domain 5B (MRF1-like) (ARID5B), mRNA.	1.61E−17
	N4BP2L1	NEDD4 binding protein 2-like 1 (N4BP2L1), transcript variant 2, mRNA.	5.05E−15
	ABTB1	Ankyrin repeat and BTB (POZ) domain containing 1 (ABTB1), transcript variant 3, mRNA.	1.32E−14
	NINJ1	Ninjurin 1 (NINJ1), mRNA.	4.48E−14
	SCG5	Secretogranin V (7B2 protein) (SCG5), mRNA.	4.94E−14
	WASPIP	Wiskott-Aldrich syndrome protein interacting protein (WASPIP), mRNA.	8.18E−14
	SIRT4	Sirtuin (silent mating type information regulation 2 homolog) 4 (S. cerevisiae) (SIRT4), mRNA.	2.26E−13
	CHODL	Chondrolectin (CHODL), mRNA.	2.55E−13
	PRTFDC1	Phosphoribosyl transferase domain containing 1 (PRTFDC1), mRNA.	3.69E−13
	PAQR8	Progestin and adipoQ receptor family member VIII (PAQR8), mRNA.	4.27E−13
	PCTP	Phosphatidylcholine transfer protein (PCTP), mRNA.	4.68E−13
	RWDD2A	RWD domain containing 2A (RWDD2A), mRNA.	4.70E−13
	BTN3A3	Butyrophilin, subfamily 3, member A3 (BTN3A3), transcript variant 2, mRNA.	6.09E−13
3	FHL2	Four and a half LIM domains 2 (FHL2), transcript variant 4, mRNA.	3.51E−22
	MIR1978	MicroRNA 1978 (MIR1978), microRNA.	9.42E−22
	ID1	Inhibitor of DNA binding 1, dominant negative helix-loop-helix protein (ID1), transcript variant 2, mRNA.	7.40E−17
	CDC25A	Cell division cycle 25 homolog A (S. pombe) (CDC25A), transcript variant 1, mRNA.	3.13E−14
	ACTB	Actin, beta (ACTB), mRNA.	3.74E−14
	WDR1	WD repeat domain 1 (WDR1), transcript variant 1, mRNA.	6.86E−14
	TMEM178	Transmembrane protein 178 (TMEM178), mRNA.	1.83E−13
	LOC440043	PREDICTED: misc_RNA (LOC440043), miscRNA.	2.17E−13
	TSKU	Tsukushin (TSKU), mRNA.	2.26E−13
	C17orf96	Chromosome 17 open reading frame 96 (C17orf96), mRNA.	2.71E−13
	POTEF	POTE ankyrin domain family, member F (POTEF), mRNA.	3.85E−13

	JUN	Jun oncogene (JUN), mRNA.	4.30E−13
	SLC7A5	Solute carrier family 7 (cationic amino acid transporter, y+ system), member 5 (SLC7A5), mRNA.	5.78E−13
	ENO1	Enolase 1, (alpha) (ENO1), mRNA.	6.82E−13
	FAM80A	Family with sequence similarity 80, member A (FAM80A), mRNA.	7.91E−13
4	LOC643031	PREDICTED: similar to NADH dehydrogenase subunit 5 (LOC643031), mRNA.	7.00E−18
	ZNF564	Zinc finger protein 564 (ZNF564), mRNA.	1.32E−17
	HSPC047	HSPC047 protein (HSPC047), mRNA.	2.83E−16
	LOC1001345 84	PREDICTED: hypothetical protein LOC100134584 (LOC100134584), mRNA.	5.32E−16
	SCGN	Secretagogin, EF-hand calcium binding protein (SCGN), mRNA.	8.23E−15
	IFNAR1	Interferon (alpha, beta and omega) receptor 1 (IFNAR1), mRNA.	8.37E−15
	SNORA25	Small nucleolar RNA, H/ACA box 25 (SNORA25), small nucleolar RNA.	1.63E−14
	ZNF606	Zinc finger protein 606 (ZNF606), mRNA.	1.98E−14
	NAPEPLD	N-acyl phosphatidylethanolamine phospholipase D (NAPEPLD), mRNA.	1.08E−13
	CLK4	CDC-like kinase 4 (CLK4), mRNA.	1.12E−13
	BCL2	B-cell CLL/lymphoma 2 (BCL2), nuclear gene encoding mitochondrial protein, transcript variant alpha, mRNA.	1.85E−13
	ZNF35	Zinc finger protein 35 (ZNF35), mRNA.	2.39E−13
	C1orf63	Chromosome 1 open reading frame 63 (C1orf63), transcript variant 1, mRNA.	3.62E−13
	COX19	COX19 cytochrome c oxidase assembly homolog (S. cerevisiae) (COX19), mRNA.	3.81E−13
	RPL23AP13	Ribosomal protein L23a pseudogene 13 (RPL23AP13), non-coding RNA.	4.93E−13

3.2. Analysis of perturbed pathways by the addition of APOM in MPP$^+$-treated SH-SY5Y cells

Pathways significantly affected by APOM might be closely related to molecular roles of APOM in MPP$^+$-treated SH-SY5Y cells. Thus, pathways significantly affected by the addition of APOM were examined with a Bioconductor package *SPIA* through signaling pathway impact analysis [20]. This analysis considered two independent probability values, P_{NDE} and $P_{PERT,}$ which were calculated for each pathway with incorporating parameters such as log2 ratios (APOM added group/reference group) of genes showing differential profiles, statistical significance of the set of pathway genes, and the topology of the signaling pathway. Two types of probability were finally combined into a global probability value, $P_{G,}$ which was used for ranking the pathways and testing the hypothesis that the pathway was significantly perturbed by APOM addition. The impact analysis was performed for 2249 significant genes that showed differential expression profiles between the APOM added group and the reference group for 135 well characterized human gene signaling pathways available in KEGG (Kyoto Encyclopedia of Genes and Genomes). Since several pathways were tested simultaneously, the significance level was set at 5% after false discovery rate (FDR) correction [24].

Three KEGG pathways (*protein processing in endoplasmic reticulum* (ER), *Fanconi anemia pathway*, and *TGF-beta signaling pathway*) showed significant perturbation at 6, 12, and 24 h after APOM treatment. It is interesting to note that the ER protein pressing pathway is affected by APOM addition because MPP$^+$ toxicity in SH-SY5Y cells might induce ER stress [16]. Table 2 shows the six
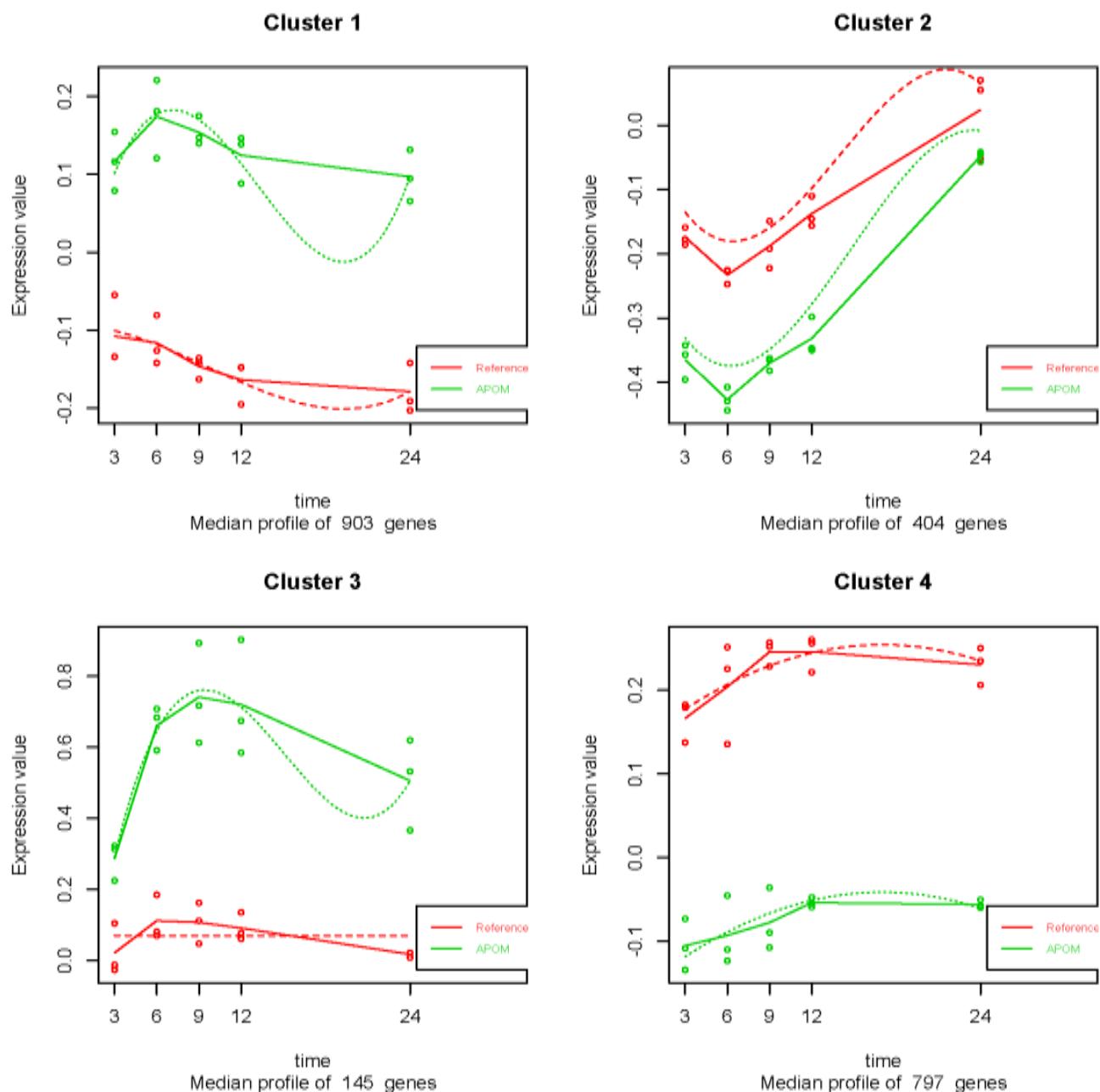
Figure 2. Average expression profiles of significant genes in four clusters of Figure 1 for the reference group and the APOM added group.

perturbed pathways detected at 12 h. Status of each pathway was determined by the total net accumulated perturbation of a given pathway, t_A, which was calculated as the sum of all perturbation accumulations for all genes in the pathway. If the value of t_A for a given pathway was negative, the pathway was considered as negatively perturbed, i.e., inhibited. On the contrary, if the value of t_A for a given pathway was positive, the pathway was considered as activated. APOM addition to MPP$^+$-treated SH-SY5Y cells resulted in the activation of three pathways (*ER protein processing*, *colorectal cancer*, and *TGF-beta signaling pathway*) and the inhibition of three pathways (*fanconi anemia*, *pathological Escherichia coli infection*, and *cell cycle*) compared to the reference group (Table 2).

Table 2. Perturbed pathways at 12 h after APOM addition to MPP⁺-treated SH-SY5Y cells.

KEGG pathway	KEGG ID	P_{size}	NDE	P_{NDE}	TA	P_{PERT}	$P_{G, FDR}$	Status
Protein processing in endoplasmic reticulum	4141	166	31	0.000	1.462	0.257	0.001	Activated
Fanconi anemia pathway	3460	52	14	0.000	−0.041	0.947	0.013	Inhibited
Colorectal cancer	5210	62	12	0.002	3.392	0.032	0.027	Activated
Pathogenic Escherichia coli infection	5130	54	12	0.000	−3.299	0.232	0.032	Inhibited
Cell cycle	4110	124	21	0.000	−2.411	0.411	0.032	Inhibited
TGF-beta signaling pathway	4350	84	11	0.044	8.516	0.004	0.037	Activated

3.3. Identification of significantly affected regions within each perturbed pathway with SEM

In the above section, pathways significantly affected by APOM addition in MPP⁺-treated SH-SY5Y cells were estimated with SPIA. Perturbed pathway may have different regulation structure between the two groups under comparison. To detect specific regions showing different regulation in each perturbed pathway, a graph model describing interactions in the pathway is useful. Since the perturbation of pathway is driven by significant genes showing differential profile between the APOM added group and the reference group, we focused on the connection of these genes. To identify how significant genes were connected in each perturbed pathway with the other genes on the microarray, the shortest paths (geodesic distance) between genes with differential profile on each perturbed pathway were searched with the function *get.shortest.paths()* of the R package *igraph* [21]. All shortest paths detected in a given pathway were merged into a graph called a shorted path model (SPM), where each node and each edge could not be presented for more than once while self-loops were excluded but feed-backs and cycles were kept. Table 3 shows the number of nodes and edges of SPMs corresponding to the six perturbed KEGG pathways shown in Table 2. Modularity and module for each SPM were detected by using the function of *walktrap.community()* of the R package *igraph*. The modularity indicates how good the division is or how separate the different vertices are from each other. A high degree of modularity indicates dense connections between the nodes within the same module but rare connections between nodes in different modules. The SPM for *cell cycle* and its module are shown in Figure 3. The connections between nodes in the same module were indicated in a black arrow while the connections between nodes in the different modules were represented by a red arrow. Each module within the SPM of the cell cycle was connected with genes such as *CDC2* and *CDC6*.

Next, we detected specific regions showing significantly different regulation in each perturbed pathway. For this, each SPM/module was evaluated with SEM to verify whether the covariance structure was significantly different between the two groups. Here, covariance structures for SPM/module were calculated from the two conditions of gene expression data, i.e., the APOM added group and the reference group. SPM/module showing significantly different covariance structures between the two groups corresponded to regions perturbed by the addition of APOM in MPP⁺-treated SH-SY5Y cells. Evaluation of covariance structure with SEM was performed against each module of SPM except for two pathways (*fanconi anemia* and *pathogenic Escherichia coli* infection) which showed very low modularity in their SPMs (Table 3).

Table 3. Modularity evaluation of shortest path models constructed from significant genes within perturbed pathways.

KEGG pathway	Original pathway (nodes/edges)	Shortest path model (nodes/edges)	Modularity of shortest path model	No. of module
Protein processing in endoplasmic reticulum	51/83	11/10	0.395	3
Fanconi anemia pathway	39/185	14/43	0.055	3
Colorectal cancer	49/106	18/22	0.458	3
Pathogenic Escherichia coli infection	40/74	4/3	0.000	4
Cell cycle	124/932	47/105	0.412	5
TGF-beta signaling pathway	73/186	11/10	0.395	3
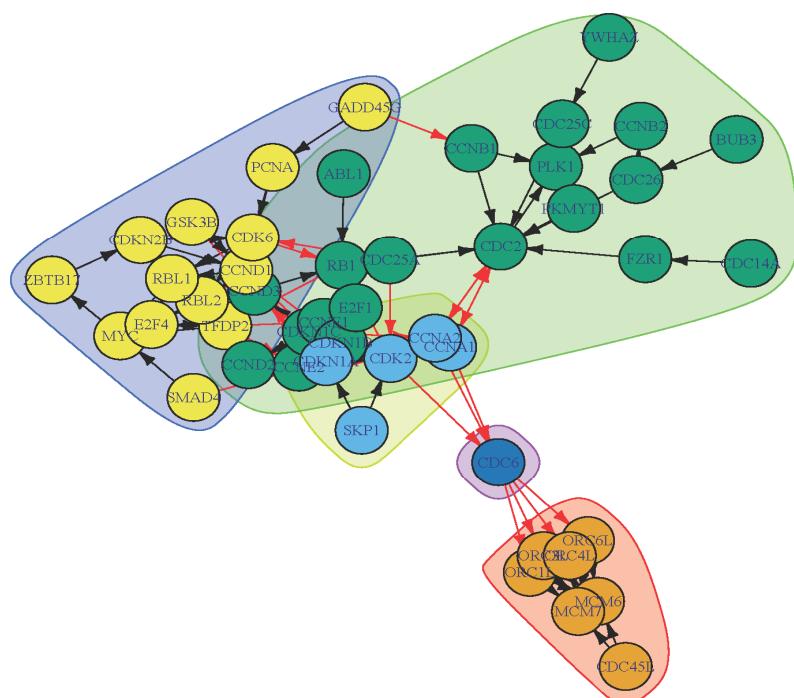
Figure 3. Five modules within the cell cycle SPM. Genes (nodes) in the same module are shown in the same color.

Evaluation of these two pathways was carried out against SPM itself and no significant difference was detected at any time points. Significant modules were detected in the other four pathways and summarized in Table 4. Module 1 of *TGF-beta signaling pathway* showed significance only at 3 h whereas module 4 of *cell cycle* showed significance at 6, 9, and 24 h. The fusion of all significant modules might provide an insight into the specific cellular mechanisms induced by APOM addition in MPP$^+$-treated SH-SY5Y cells. Figure 4 shows the union of all significant modules in Table 4. The yellow and green nodes represent significant genes and non-significant genes within modules, respectively. The total number of genes on the graph of Figure 4 was 47, including 18 significant genes and 29 non-significant genes. Although non-significant genes did not show differential expression

profile between the APOM-added group and the reference group, they might have important role as signal mediator when they are connected directly or indirectly to significant genes.

To examine the association of these 47 genes with disease, enriched disease ontology (DO) terms were investigated with the function *enrichDO()* of the R package *DOSE* [25]. DO analysis against these 47 genes detected many significant DO terms such as DOID:0060116 (sensory system cancer, q-value = 1.52×10^{-15}), DOID:768 (retinoblastoma, q-value = 6.07×10^{-14}), and DOID:769 (neuroblastoma, q-value = 6.99×10^{-6}). Most of the enriched DO terms were related to cancer.

Table 4. Significant modules detected by covariance analysis with SEM for the four shortest path models.

Shortest path model	Time (h)				
	3	6	9	12	24
Protein processing in endoplasmic reticulum	-	-	Module 1	Module 3	Module 3
Colorectal cancer	Module 2	Module 2	-	-	-
Cell cycle	-	Module 4	Module 3, 4	Module 3	Module 4
TGF-beta signaling pathway	Module 1	-	-	-	-
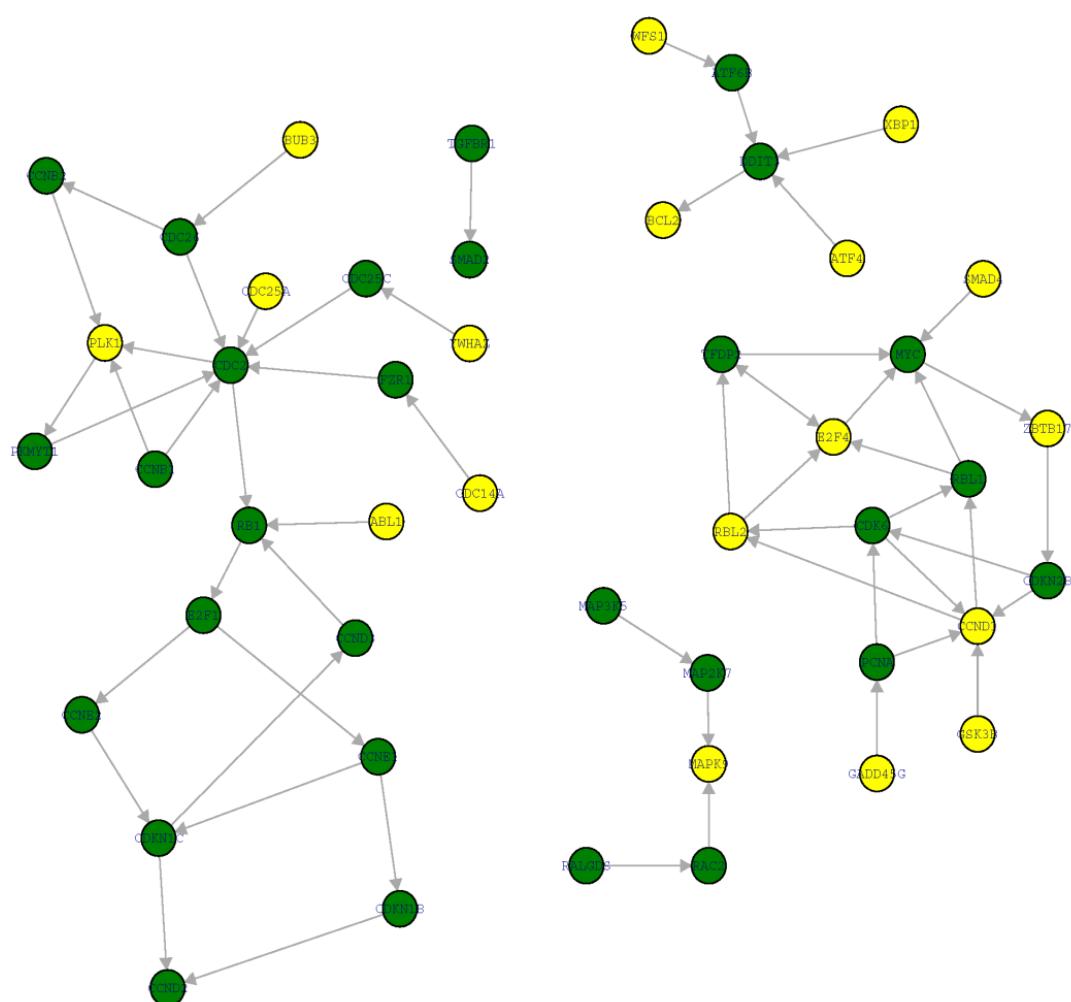
Figure 4. Merged graph of significant regions. Yellow and green colors represent significant and non-significant genes, respectively.

This indicates that APOM might induce the expression change of cancer related genes to overcome the toxicity of MPP$^+$. Figure 5 shows the expression profiles of 18 significant genes shown in Figure 5. The red color and the green color represent the reference and the APOM added group, respectively. The expression profile of *BCL2* showed clear contrast between the two groups. It showed a time-dependent increase in the reference group but a time-dependent decrease in the APOM added group. This indicates that APOM may be able to induce the inhibition of *BCL2* in MPP$^+$-treated SH-SY5Y cells. Genes such as *CDC14A*, *RBL2*, and *SMAD4* tended to be up-regulated in the reference group while genes such as *ABL1*, *GADD45G*, and *GSK3B* tended to be up-regulated in the APOM added group.
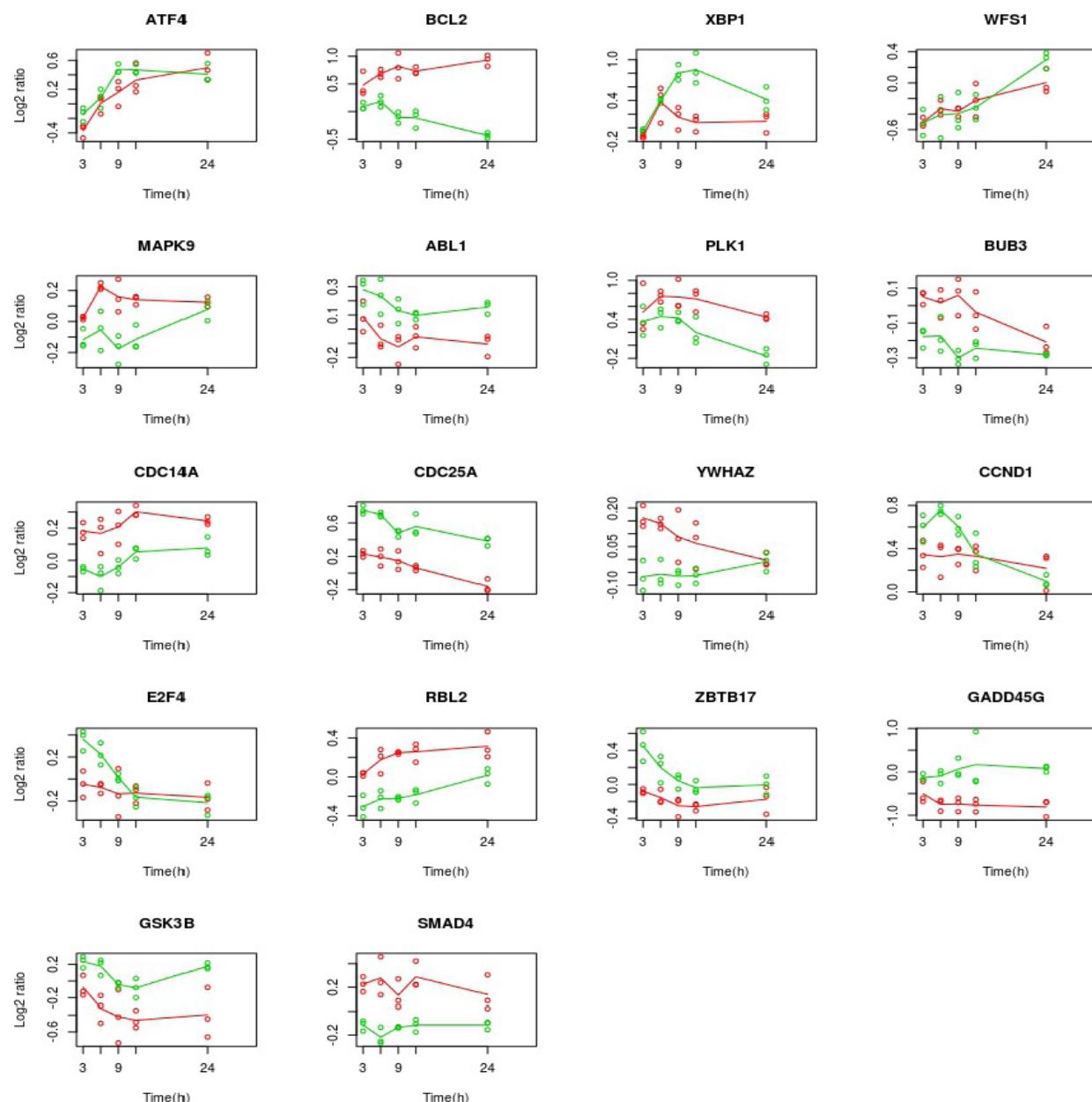
Figure 5. The expression profiles of significant genes (yellow nodes) in the network shown in Figure 4. Red and green lines represent average expression profiles of the reference and APOM added groups, respectively. The expression values of replicates were indicated with three circles (○) at each time point.

4. Discussion and Conclusion

The antiparkinsonian effect of APOM on PD patients is similar to that of levodopa. However, different from levodopa, APOM does not require decarboxylation to be activated. That is, levodopa needs to be converted into dopamine to be effective for PD, whereas APOM is readily diffused across the blood-brain barrier, directly playing a role as non-selective dopamine agonist. Besides its receptor-mediated action, APOM functions as a potent antioxidant and free radical scavenger [9,10]. Currently, APOM is used for treating advanced PD patients who do not respond to levodopa or other dopamine agonists [26]. However, side effects such as orthostatic hypotension, nausea, and fibrotic nodules at the site of APOM injection have been reported after long-term use of APOM for treatment of PD patients [2]. To secure the use of APOM in PD treatment, it is essential to understand the molecular mechanism involved in its effect. In this study, genome-wide gene expression profiles were examined at several time points after the addition of APOM to a PD cell model, i.e., MPP^+-treated human neuroblastoma SH-SY5Y cells. They were compared to those of PD cell model without APOM treatment. Among a total of 32,421 genes, 2249 genes showed significantly different expression profiles between the APOM added group and the reference group. These 2249 genes were divided four clusters (Figure 1). Genes of cluster 1 were up-regulated in the APOM added group but down-regulated in the reference group. GO enrichment analysis against genes of cluster 1 showed enrichment of GO terms such as GO:0036297 (interstrand cross-link repair) and GO:0022616 (DNA strand elongation). This suggests that APOM might provide protective mechanism against DNA damage induced by MPP^+ toxicity. The up-regulation of genes in cluster 3 indicated that APOM could activate the metabolic process because GO terms such as GO:0009185 (ribonucleoside diphospahte metabolic process), GO:0019320 (hexose catabolic process) and GO:0006096 (glycolytic process) were enriched in cluster 3.

To systematically investigate the role of significant genes in cells, significantly affected pathways by APOM addition were explored with SPIA. Significant perturbation at 6, 12, and 24 h was found for the following three KEGG pathways: *protein processing in endoplasmic reticulum* (ER), *Fanconi anemia pathway*, and *TGF-beta signaling pathway*. To detect specific regions with differential regulation of each perturbed pathway, SPM/module constructed with significant genes were evaluated with SEM. Significant modules were detected from SPMs for the following four pathways: *ER protein processing*, *colorectal cancer*, *cell cycle*, and *TGF-beta signaling pathway* (Table 4). As significant modules may reflect the effect of APOM on PD cells in terms of molecular interaction, identification of them will be important for understanding the molecular mechanism involved in the action of APOM. The fusion of all significant modules consisting of 18 significant genes and 29 non-significant genes was shown in Figure 4. Non-significant genes connected to significant genes might have important role as signal mediators. DO analysis against these 47 genes detected many enriched DO terms, most of which were related to cancer. This suggests that APOM might induce changes in the expression of some cancer related genes for survival from MPP^+-induced neuronal toxicity. Crosstalk among these 47 genes might improve our understanding of the molecular mechanism involved in the effect of APOM on PD.

Conflicts of Interest

The author declares no conflict of interest.

References

1. Ribarič S (2012) The pharmacological properties and therapeutic use of apomorphine. *Molecules* 17: 5289-5309.
2. Deleu D, Hanssens Y, Northway MG (2004) Subcutaneous apomorphine: an evidence-based review of its use in Parkinson's disease. *Drugs Aging* 21: 687-709.
3. Sydow O (2008) Parkinson's disease: recent development in therapies for advanced disease with a focus on deep brain stimulation (DBS) and duodenal levodopa infusion. *FEBS J* 275: 1370-1376.
4. Haeri M, Sarbaz Y, Gharibzadeh S (2005) Modeling the Parkinson's tremor and its treatments. *J Theor Biol* 236: 311-322.
5. Antonini A, Isaias IU, Rodolfi G, et al. (2011) A 5-year prospective assessment of advanced Parkinson disease patients treated with subcutaneous apomorphine infusion or deep brain stimulation. *J Neurol* 258: 579-585.
6. Carron R, Fraix V, Maineri C, et al. (2011) High frequency deep brain stimulation of the subthalamic nucleus versus continuous subcutaneous apomorphine infusion therapy: A review. *J Neural Transm* 118: 915-924.
7. De Gaspari D, Siri C, Landi A, et al. (2006) Clinical and neuropsychological follow up at 12 months in patients with complicated Parkinson's disease treated with subcutaneous apomorphine infusion or deep brain stimulation of the subthalamic nucleus. *J Neurol Neurosurg Psychiatry* 77: 450-453.
8. Merello M, Lees AJ, Balej J, et al. (1999) GPi firing rate modification during beginning-of-dose motor deterioration following acute administration of apomorphine. *Mov Disord* 14: 481-483.
9. Gassen M, Glinka Y, Pinchasi B, et al. (1996) Apomorphine is a highly potent free radical scavenger in rat brain mitochondrial fraction. *Eur J Pharmacol* 308: 219-225.
10. Grunblatt E, Mandel S, Gassen M, et al. (1999) Potent neuroprotective and antioxidant activity of apomorphine in MPTP and 6-hydroxydopamine induced neurotoxicity. *J Neural Transm Suppl* 55: 57-70.
11. Do JH (2014) Neurotoxin-induced pathway perturbation in human neuroblastoma SH-EP cells. *Mol Cells* 37: 672-684.
12. Kim IS, Choi DK, Do JH (2013) Genome-wide temporal responses of human neuroblastoma SH-SY5Y cells to MPP$^+$ neurotoxicity. *BioChip J* 7: 247-257.
13. Nakamura K, Bindokas VP, Marks JD, et al. (2000) The selective toxicity of 1-methyl-4-phenylpyridinium to dopaminergic neurons: The role of mitochondria complex I and reactive oxygen species revisited. *Mol Pharmacol* 58: 271-278.
14. Lotharius J, O'Malley KL (2000) The parkinsonisminducing drug 1-methyl-4-phenylpyridinium triggers intracellular dopamine oxidation. A novel mechanism of toxicity. *J Biol Chem* 275: 38581-38588.
15. Moon HE, Paek SH (2015) Mitochondrial dysfunction in Parkinson's disease. *Exp Neurobiol* 24: 103-116.
16. Choi DK, Kim IS, Do JH (2014) Signaling pathway analysis of MPP+-treated human neuroblastoma SH-SY5Y cells. *Biotechnol Bioprocess Eng* 19: 332-340.

17. Du P, Kibbe WA, Lin SM (2008) Lumi: a pipeline for processing Illumina microarray. *Bioinformatics* 24: 1547-1548.
18. Conesa A, Nueda MN, Ferrer A, et al. (2006) maSigPro: a method to identify significantly differential expression profiles in time-course microarray experiments. *Bioinformatics* 22: 1096-1102.
19. Yu G, Wang LG, Han Y, et al. (2012) clusterProfiler: an R package for comparing biological themes among clusters. *Omics* 16: 284-287.
20. Tarca AL, Draghici S, Khatri P, et al. (2009) A novel signaling pathway impact analysis. *Bioinformatics* 25: 75-82.
21. Csárdi G, Nepusz T (2006) The igraph software package for complex network research. *Inter J Complex Syst* 1695.
22. Pepe D, Do JH (2015) Estimation of dysregulated pathway regions in MPP+ treated human neuroblastoma SH-EP cells with structural equation model. *BioChip J* 9: 131-138.
23. Newman ME, Girvan M (2004) Finding and evaluating community structure in networks. *Phys Rev E Stat Nonlin Soft Matter Phys* 69: 026113.
24. Benjamini Y, Yekutieli D (2001) The control of the false discovery rate in multiple testing under dependency. *Ann Stat* 29: 1165-1188.
25. Yu G, Wang KG, Yan GR, et al. (2015) DOSE: an R/Bioconductor package for disease ontology semantic and enrichment analysis. *Bioinformatics* 31: 608-609.
26. Okun MS, Foote KD (2010) Parkinson's disease DBS: what, when, who and why? The time has come to tailor DBS targets. *Expert Rev Neurother* 10: 1847-1857.